Advances in Industrial and Manufacturing Engineering 2 (2021) 100039

Contents lists available at ScienceDirect

Advances in Industrial and Manufacturing Engineering

journal homepage: www.journals.elsevier.com/advances-in-industrial-and-manufacturing-engineering

Soft sensor approach based on magnetic Barkhausen noise by means of the forming process punch-hole-rolling

F. Mühl [a,*], M. Knoll [b], M. Khabou [a], S. Dietrich [a], P. Groche [b], V. Schulze [a]

[a] Institute for Applied Materials - Material Science, KIT Karlsruhe, Germany
[b] Institute for Production Engineering and Forming Machines, Technical University of Darmstadt, Germany

ARTICLE INFO

Keywords:
Magnetic barkhausen noise
Soft sensor
Surface treatment
Metal forming
Property control
Punch-hole rolling

ABSTRACT

The relevance of the magnetic Barkhausen noise (MBN) and the non-destructive characterization of material properties in near surface layers, has increased in recent years.With the development of new signal processing techniques, the method was further developed into a powerful evaluation technique and is used in various areas of online and offline measurement. In addition to the established use in the detection of grinding burn, the method is increasingly used in the context of soft sensors for property controlled processes, due to its short analysis times. By a detailed description of a soft sensor concept for the novel forming process punch-hole-rolling this work focuses on the offline characterization of the process specific cause-effect relationships. This is done by analyzing the process interactions as well as the surface layer state by a metallographic investigation. Additionally a non-destructive characterization by means of MBN was done and correlated with the surface layer state. This provides important findings for the use of a MBN-sensor in a soft sensor concept and the potential integration into the forming process.

1. Introduction and state of the art

In the recent years soft sensors became a useful tool in industrial application (Kadlec et al., 2009; Fortuna et al., 2007; Ahmad et al., 2014a, 2014b). Especially their ability of real-time estimation of important process information, which cannot be analysed by a physical sensor itself, can improve the process control and also reduce time consuming off-line sample analyses (Fortuna et al., 2007). In general a soft sensor is a combination of a physical sensor and mathematical models, which describe correlations of variables from different physical fields (Schulze et al., 2020). Soft sensor models can be divided into three classes, namely white-box models (WB), grey-box models (GB) and black-box models (BB). White-box models utilize physical models, whereas grey-box models are based on multivariate statistics and phenomenological correlations (Fortuna et al., 2007; Ahmad et al., 2020; Sohlberg, 2005). Observers that are commonly used in control engineering belong to white-box models, such as the Kalman filter (Kadlec et al., 2009). With increasingly complex models the use of artificial intelligence in the soft-sensor is put forward and forms the basis of so-called black-box models. By integrating a soft sensor concept in manufacturing processes for the estimation of component properties, a higher process stability as well as a higher degree of automation can be achieved (Mulrennan et al., 2018). In addition, an in-line determination of product properties like hardness, residual stresses and microstructure enables property controlled processes and also a direct compensation of disturbances arising e.g. due to material fluctuations and the wear of tools. This concept requires the knowledge of an accessible variable, which can be correlated with the desired inaccessible product property using suitable models based on process knowledge with a certain complexity. The known variables used in the models can be derived from different process parameters or measurable material properties. Considering a soft sensor based on material properties from non-destructive (NDT) measurement techniques the respective measurements have to correlate with the above mentioned typical product property or characteristic of the surface layer state. The most common methods are hereby electromagnetic techniques like the eddy current method (Abu-Nabah et al., 2009; García-Martín et al., 2011; Zergoug et al., 2004) and Barkhausen noise measurements (Boller et al., 2011; Stefanita, 2008) using electromagnetic induction fields for the surface characterization. In metal forming of steel components the implementation of such soft sensors for an increase of process stability and degree of automation is not widely realized and only a few concepts are described in literature (Heingärtner and Hora, 2011). In contrast to that for machining processes different soft sensor approaches dealing with the surface layer state have already been developed and

* Corresponding author.
E-mail address: fabian.muehl@kit.edu (F. Mühl).

https://doi.org/10.1016/j.aime.2021.100039
Received 28 January 2021; Received in revised form 11 March 2021; Accepted 29 March 2021

evaluated (Meurer et al., 2020; Böttger et al., 2020; Jedamski et al., 2020). In (Meurer et al., 2020) a soft sensor concept estimating the formation of white layers during hard machining is presented. Hereby the in-line measurement of cutting forces in combination with a heuristic model estimation of the temperature field was used to estimate the depth of arising white layers. The results of the soft sensor showed a promising correlation with the results from a time consuming FE-model and experimental investigations indicating the potential of soft-sensors in real-time monitoring and control. In (Böttger et al., 2020) and (Jedamski et al., 2020) electromagnetic properties were used as input signal for a soft sensor concept detecting white layer transformation during turning and changes in hardness during grinding respectively. In both works the suitability of the magnetic Barkhausen noise (MBN) as a part of a soft sensor concept for predicting relevant product properties was illustrated.

1.1. Magnetic Barkhausen noise analysis

The magnetization of ferromagnetic materials is characterized by the growth of magnetic domains and thus the movement of domain walls, which separate domains with different magnetic orientation. The movement of the domain walls can be detected by sudden discontinuous change in magnetization, which is provoked by the interaction of domain walls with pinning sites from material defects. During a cyclic magnetization this effect, the so called Barkhausen noise, can be detected and evaluated by measuring the magnetic flux density B of the material. Due to the fact that the domain wall movement interacts with microstructural characteristics, the characteristic Barkhausen noise as well as the magnetization behaviour, described by the remanence M_R and the coercivity H_c, are sensitive to the material state. Hereby, the magnetic material response depends on grain size, precipitations, alloying elements, dislocations and also residual stresses, which constitute pinning sites for the domain wall movement (Fortuna et al., 2007; Le Manh et al., 2020; Sakamoto et al., 1987; Gatelier-Rothea et al., 1998; Ranjan et al., 1987). In literature, the most sensitive Barkhausen noise specific measuring parameters are the root mean square (RMS) value and the amplitude as well as the number of events of the Barkhausen noise. Generally it can be said that lattice effects like dislocations, grain boundaries and foreign atoms increasing materials hardness will increase the mentioned Barkhausen noise parameters as well as the coercivity of the material (Fortuna et al., 2007; Stefanita, 2008; Baak et al., 2019), whereas compressive/tensile residual stresses will decrease/increase the Barkhausen noise by a simultaneous increase/decrease of the coercitivity due to magnetostriction (Fortuna et al., 2007; Žerovnik and Grum, 2009). The mutual influence of the microstructural effects and their sensitivity is a complex interplay and therefore a quantitative Barkhausen noise evaluation has to base on material specific calibration measurements and take place under controlled conditions. Nevertheless the measurement technique is suited to identify fluctuations as well as process instabilities in a non destructive manner in manufacturing processes (Fortuna et al., 2007).

1.2. Punch-hole-rolling

The punch-hole-rolling process is a combination of a conventional punch process and the subsequent hole-rolling process. The process can be carried out in one tool or on two separate tools as well as on two different machines. The shear surface created during the punch process, with its typical shearing surface, draw-in, breakage and burr zone, is reshaped during the subsequent hole-rolling process by the incremental workpiece to tool contact. Thereby a continuous radial as well as rotational relative movement between tool and workpiece takes place. Due to the continuous process of the hole-rolling process, a plastic smoothing of the shear surface occurs at the beginning of the process. As the plastic forming progresses, the material splits into a double sided collar similar to flow splitting or rotational splitting of disk blanks (Groche et al., 2007; Schmoeckel and Hauk, 2000). The dependence of the flow curve k_f on strain ε, strain rate $\dot{\varepsilon}$ and temperature T makes it possible to produce different collar heights with the same initial punch diameter and sheet thickness by means of targeted process control. The current experimental setup is based on a conventional lathe and is carried out in two steps, see Fig. 1. Thereby, the spindle drive is used to rotate the workpiece and the slide to realise the radial feed, as described in (Knoll et al., 2020).

1.3. This work

The aim of this study was to set up a soft sensor concept dealing with component geometry and product properties by incorporating a closer look into the forming process punch-hole-rolling and its microstructure development. This was achieved by an experimental parameter study concentrated on the characterization of the resulting surface layer state. Based on the investigated process-property relationship a soft sensor approach estimating component properties is described. Furthermore the use of an MBN measuring system *Rollscan350* capable of in-process measurements manufactured by *Stresstech* was tested with regard to realizable measuring parameters, working distance and also the microstructure sensitivity.

2. Process and material knowledge

The punch-hole-rolling process has mainly two control variables, which can be adjusted during forming. The rotation speed n as well as the radial feed rate $\dot{r}$. The process interactions of these parameter was studied by varying the rotational speed n between 25 rpm and 800 rpm and the radial feed rate $\dot{r}$ between 0.03 mm/round and 0.2 mm/round respectively. The deduced deformation speed v_d varies between $0.0125\mathrm{mms}^{-1}$ and $1.3\mathrm{mms}^{-1}$. Starting from a drilled hole with a diameter of 8.2 mm, the samples were widened to different end diameters. Hereby the development of the surface layer state and the component properties were observed. As testing material a sheet steel 1.0338 with outer dimensions 100 mm x 100 mm, a thickness of 2 mm, a yield strength of 208 MPa and a tensile strength of 318 MPa was used. The material used has an initial grain size of 16 μm and a hardness of 110 HV1. The initial punched samples as well as the ferritic microstructure are depicted in Fig. 2.

2.1. Process-property interactions

For this study 252 experimental samples were processes on a conventional lathe to analyse the radial feed rate and rotation speed effect in the punch-hole-rolling process. Therefor the radial feed rate and the rotational speed of the lathe were varied. For each radial feed rate to rotational speed combination, three samples with a final inner diameter between 10 mm and 20 mm were produced in 2 mm steps. The start and stop of the process is realised by the operator, which causes the final diameters achieved to be subject to small fluctuations. Afterwards, the achieved inner diameter and the collar height were measured with a

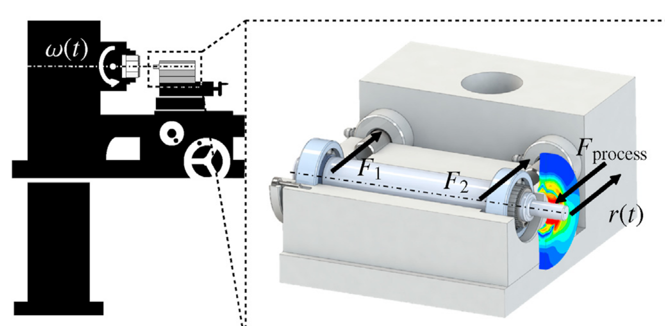

Fig. 1. Experimental process setup on a conventional lathe (Knoll et al., 2020).

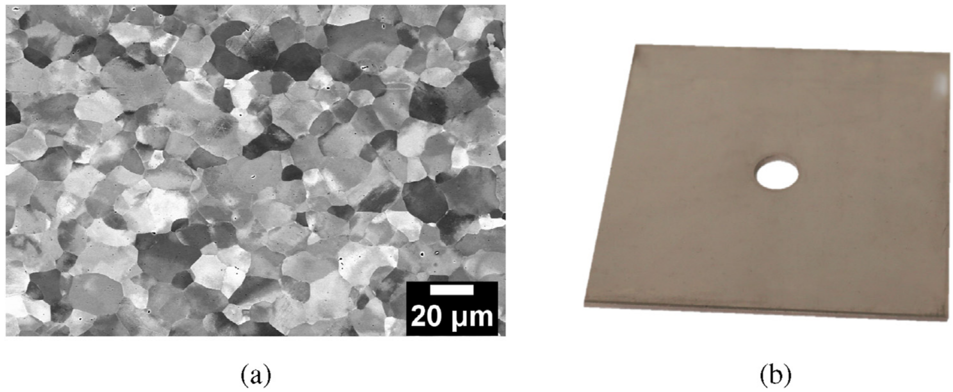

Fig. 2. a) SEM image of the initial ferritic microstructure of the sheet steel 1.0338 with a hardness of 110 HV1 and b) the initial sample condition with a 8 mm punch hole.

caliper gauge. The same test set-up and post-process as described in (Knoll et al., 2020) were used to measure the force and tool path. In addition to the force and the tool path, the temperature on the outer surface of the collar was added to the measuring system. To measure the temperature, a pyrometer CTLT25FCF from *Optris* was used. For that purpose the surface of the sample facing the pyrometer had to be coated in black thermal paint for the temperature measurement so that a consistent measurement quality is achieved.

The influence of the variable speeds can be assessed using the force-displacement and collar height to inner radius curves depicted in Fig. 3 and Fig. 4. Fig. 3 shows, that the process force increases with increasing radial feed rate. The increase in the process force results from a material deformation and surface contact effects. First and foremost, the material to be formed per revolution increases with increasing radial feed rate while also the flow stress increases with the higher strain rate. Additionally there is a contribution from material hardening. Secondly, continuously increasing collar height with increasing inner radius r_i, leads to an increasing process force due to the increasing contact surface. A deeper analysis of the experiments also indicates that the rotational speed has a negligible influence on the resulting process force, which is lost in the measurement noise.

In Fig. 4, the resulting collar heights of all samples are summarised with respect to the radial feed rates. It can be seen, that the relation between feed rate and collar height follows a similar trend as the relation between feed rate and process force. The small variations in the collar height and inner radius can be attributed to the measurement method and the inaccuracy of the pre-hole production with drilling operations,

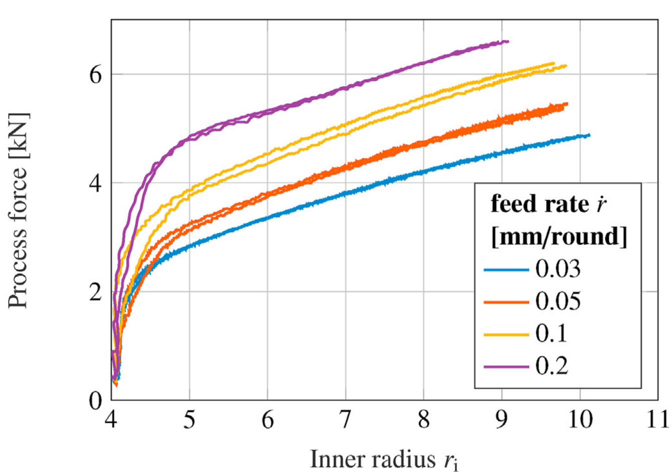

Fig. 3. Measured radial process force depending on radial feed rate and inner tool radius. Two example measurements for each feed rate with a rotational speed of 50 rpm.

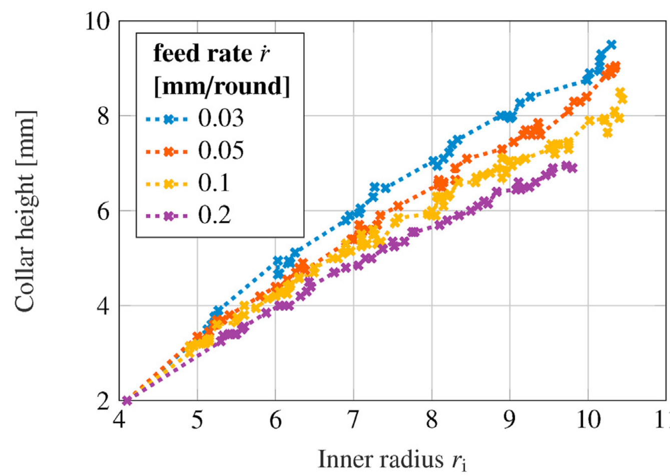

Fig. 4. Influence of different feed rates on the resulting collar height at rotation speeds between 25 rpm and 210 rpm.

which lie within ±0.1 mm. Analogously to the process forces the variation of the rotational speed can not be determined. In contrast to the collar height and process force, temperature differences can be detected when the rotational speed changes. The temporal temperature measurement is therefore a relevant measurement parameter for a model in a soft sensor.

The measured temperature differences $\Delta T = T_{end.} - T_{start}$ which can be achieved by the process are in the range between 4 K and 110 K. The temperature of the collar depends on the deformation speed. The maximum temperature of the test series is reached at an feed rate of $\dot{r} = 0.1$ mm/round and a rotational speed of $n = 800$ rpm.

2.2. Surface layer state

The highly deformed collars were produced without cracks up to the investigated inner diameter of 26 mm. A light microscopy image of a collar cross section at a diameter of 18 mm after a deformation speed with $v_d = 0.0125\text{mms}^{-1}$ is depicted in Fig. 5a. It can be seen that punch-hole-rolling leads to a nearly symmetric collar with a straight smooth surface over the complete collar height. The associated surface near SEM-Image (Fig. 5b), resolving the grain size distribution, shows a highly deformed region up to a depth of around 1.8 mm with a transition into the initial globular ferritic microstructure. The microstructure at the surface in the middle of the collar shows a banded structure with a high aspect ratio parallel to the surface. This indicates a dominant material flow in axial direction due to the high radial compressive stresses during the process (see (Knoll et al., 2020).). With decreasing radial stresses and

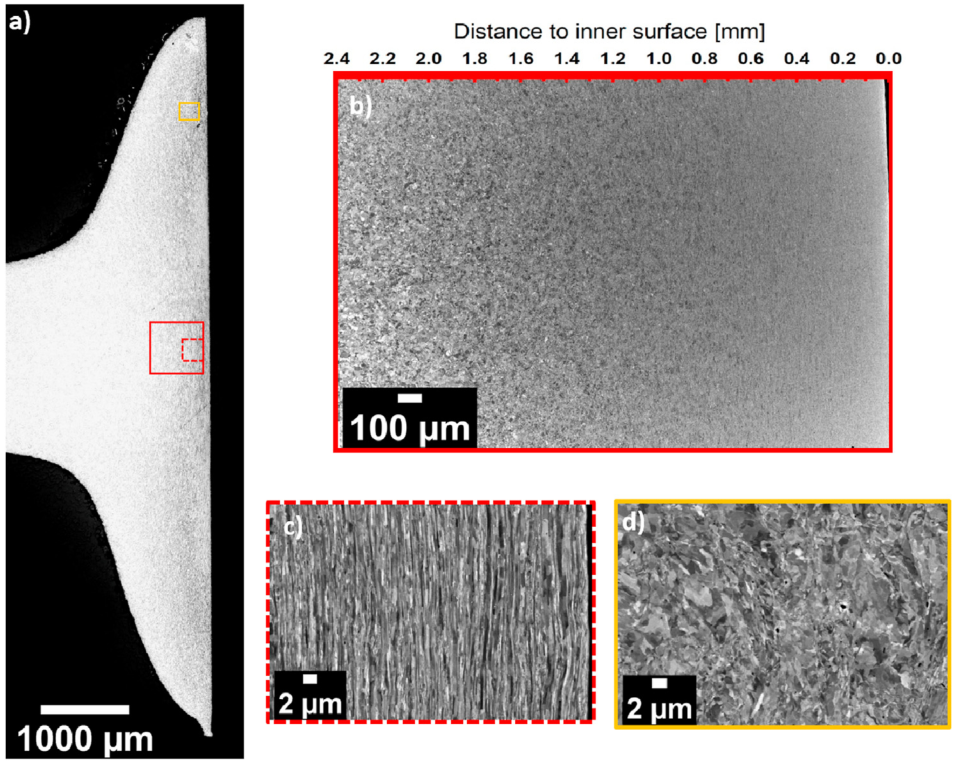

Fig. 5. Collar geometry (a) and the resulting surface microstructure at a diameter of 18 mm after rolling with a rotational speed S of 25 rpm and a feed rate $\dot{r}$ of 0.03mms^{-1}. (b) Overview of the microstructural gradient and microstructure at the surface in the middle (c) and the tip (d) of the collar.

supporting effects in the tip of the collar the grain structure changes into a globular shape, which can be seen in Fig. 5d. Nevertheless both high resolution micrographs of the surface in Fig. 5 show an ultrafine-grained (UFG) microstructure with grain sizes lower than 1 μm.

The UFG microstructure is typical for severe plastic deformation processes e.g equal channel angular extrusion (ECAP), linear flow splitting or high-pressure torsion (HPT). Considering the material flow along the induced surface, punch-hole rolling is similar to the process of linear flow splitting, where sheet metals are highly deformed by splitting the sheet in two flanges and the degree of deformation is not limited by the plastic deformability due to the induced grain refinement with its formation of dislocation cell structures. Hereby a steady state in the process

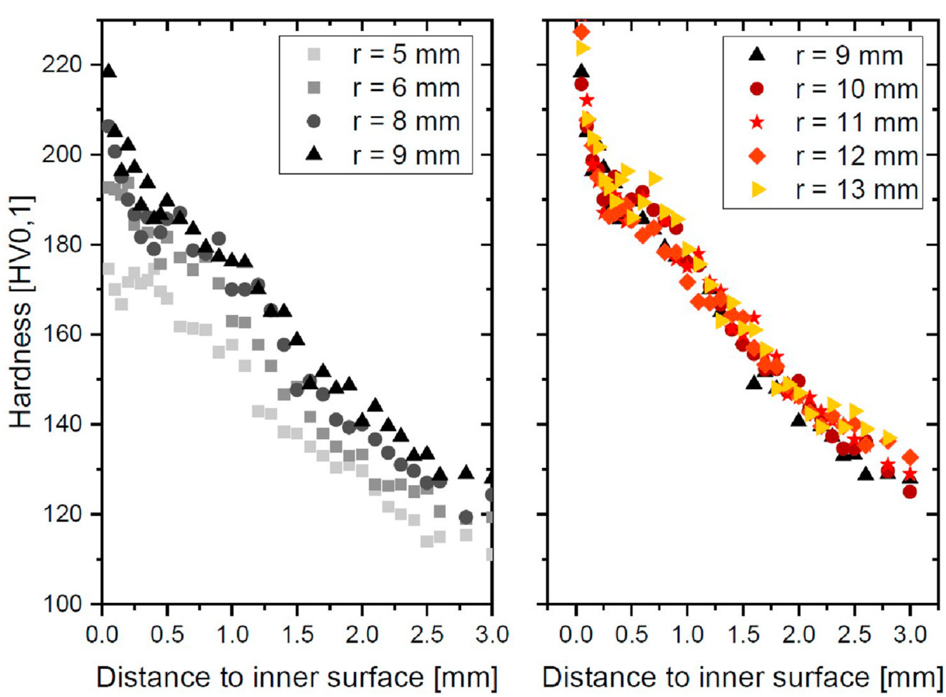

Fig. 6. Hardness distribution in dependence of the degree of deformation at a deformation speed v_d of 0.0125mms^{-1} for small radii (left) and higher radii with UFG formation (right).

zone with a UFG microstructure and constant dislocation density is achieved. The measured hardness distributions in the middle of the collar cross-section in Fig. 6 confirm the findings from (Müller et al., 2007). Up to a inner radius of 9 mm an increasing surface hardness can be detected, which can be explained by the occurring grain refinement as well as the increasing dislocation density. The hardness decreases up to a depth of 2 mm reaching the initial hardness, which correlates with the microstructural gradient in Fig. 5b. The plastically deformed depth increases also up to a depth of 9 mm and remains constant along with the maximum surface hardness at higher degrees of deformation (Fig. 6 right) indicating a steady state despite of increasing deformation. Another characteristic in the hardness distribution is the sharp decrease of the surface hardness in the first 250 μm. Afterwards a plateau of the hardness up to 1 mm followed by a smooth decrease up to the initial hardness is evident. Especially at lower radii only the plateau without a sharp increase can be detected and the plateau hardness increases with increasing deformation up to 190 HV, indicating a saturation of the occurring deformation induced dislocation density. With higher deformation degrees the formation of UFG microstructure starts and the hardness reaches its maximum with 230 HV.

As can be seen in Fig. 7, the surface hardness as well as the plastically deformed depth are independent of the used feed rate $\dot{r}$. The surface hardness shows a nearly linear increase with increasing inner radius up to 11 mm and 230 HV and remains constant with higher deformations.

3. Soft sensor approach

The primary goal of the soft sensor concept is to measure product properties such as Vickers hardness HV, grain size d, surface quality R_z and collar height $H_{coll.}$, which cannot be measured online in the process. Furthermore, disturbance variables such as fluctuations in semi finished products, material quality or wear of the tool can be detected and compensated in the process. Hereby, several information gained by different sensors combined with extensive process, material and simulation knowledge, have to be processed and linked together. An approach for the integration and interaction of a soft sensor in the process of punch-hole-rolling, enabling a property controlled process is shown in Fig. 8. In order to ensure an accurate prediction of the desired product properties, the interactions of process parameters and product properties must be correlated via online and offline analysis as well as simulation approaches. Finally, models must be derived serving as measuring functions for the soft sensor to supply previously inaccessible information about product properties, which can not be directly measured online by a sensor. In the context of punch-hole-rolling, the most important properties correlating with the process parameters are the surface layer states characterized by hardness, residual stresses and grain size, as well as geometry and surface quality. Besides final product properties also the effects of process and material fluctuations have to be considered. Especially the initial grain size d_0 and hardness HV_0, which can be determined in advance by non-destructive MBN-characterization, as well as sheet thickness s_0, tensile strength R_m and yield strength R_e can be included as influencing variables in the measurement function. Altogether, the measurement functions make use of a variety of data from different physical domains and combine them to predict the actual product properties. In the context of punch-hole-rolling four different, process integrated, physical sensors are used, namely a force-, temperature-, displacement- and especially a MBN-sensor. The MBN-sensor, in this context, is able to provide hitherto untapped information about the material condition due to its measurement location and physical principle. The input parameters for the sensor comprise the machine parameters n and $\dot{r}$, the radial process force F_r, the deformation radius r, the temperature T as well as the MBN specific parameters $MBN_{param.}$. Out of this data collection, the target variables hardness HV, grain size d, surface quality R_z and collar height $H_{coll.}$ are then predicted with suitable models (see Equation (1)). In the next step the model results are transferred to the controller, which in turn converts them based on the process into modifiable machine control parameters. Hereby a so called on-line closed-loop control can be achieved (Allwood et al., 2016). This requires a prior detailed process characterization as well as a calibration of the physical sensors. With regard to the MBN sensor, extensive offline experiments have to be carried out to locate and classify all influencing variables and material effects in the MBN signal. This process is describe in detail in the next section.

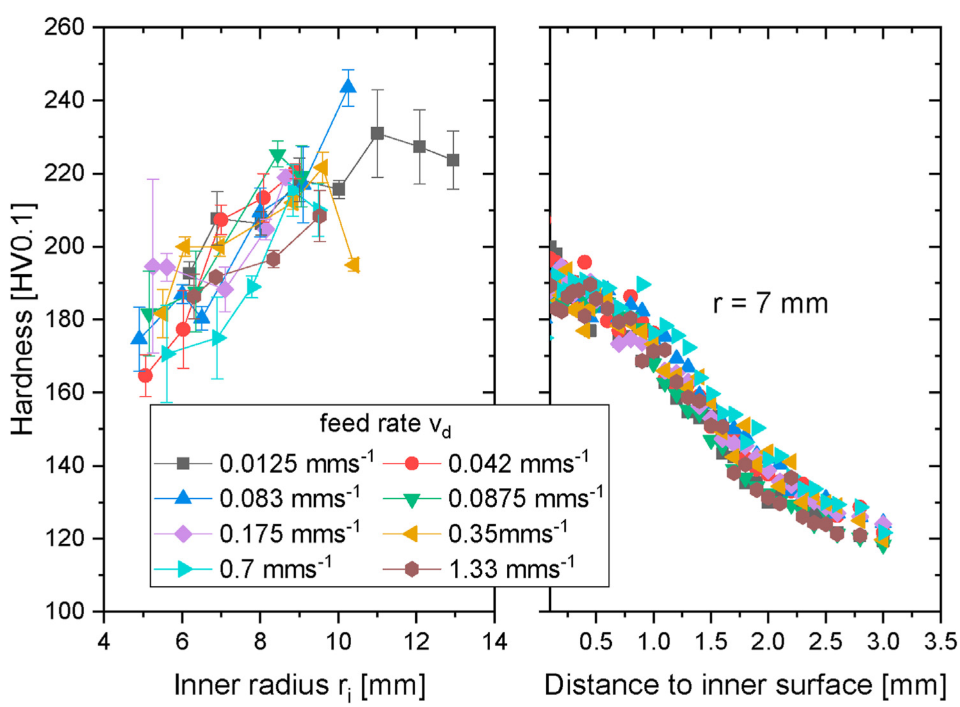

Fig. 7. Hardness 50 μm underneath the surface in dependence of the feed rate $\dot{r}$ at different states of deformation (left); hardness distribution at a widening radius of 7 mm for different deformation speed v_d (right).

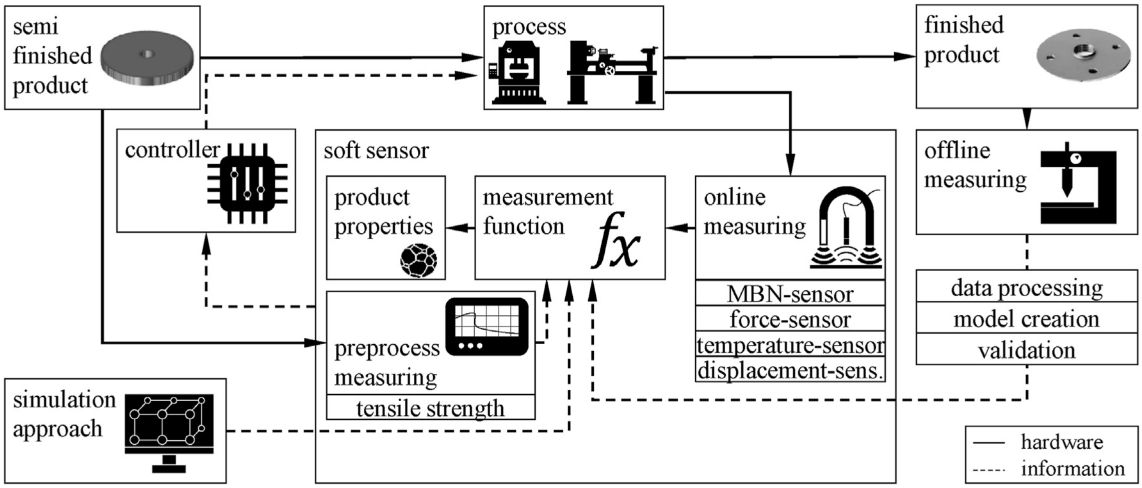

Fig. 8. Measured radial process force depending on radial feed rate and inner tool radius. Two example measurements for each feed rate.

$$HV, d, R_z = f\left(\dot{r}, n, Fr, T, MBN_{\text{param.}}, HV_0, d_0\right)$$
$$H_{\text{Col.}} = f\left(r, \dot{r}, n, F_r, T, s_0, d_0, R_z, R_e\right) \quad (1)$$

4. Magnetic Barkhausen noise analysis

The punch-hole rolled samples were investigated with a *Rollscan350* Barkhausen noise analyzer manufactured by *Stresstech* with a focus on the surface microstructure. The results were evaluated with the MBN software *MicroScan*, providing the RMS value, maximum amplitude, number of counts and the characterization of the MBN envelope by the peak position as well as the full width at half maximum (FWHM). A cylindrical sensor, inducing a magnetization in z-direction of the collar, was used for the investigations on the round inner surface. The sensor unit with a height of 7.5 mm consists hereby of two exitation coils and one isolated detection coil in the middle. In order to set the contact conditions or the distance between sensor and surface as accurately and reproducible as possible, the specimens were fixed on an adjustable xyz-table, including a micrometer screw in every direction. Furthermore, a strain gauge was used on the sensor holder to detect the contact between the sensor and the surface. The experimental setup and the sensor concept are shown in Fig. 9. The MBN characterization was carried out using two parameter sets of magnetization frequency f_M and voltage V_M. On the one hand the manufacturer's recommended standard frequency of 125 Hz with a magnetization voltage of 9 V was used. On the other hand a lower frequency with 50 Hz, leading to more extensive penetration depths, in combination with a high magnetization voltage of 16 V was tested. Additionally, the gap between sensor and surface was investigated to evaluate the process integratability of a MBN-Sensor.

The RMS values obtained with both measurement settings after different states of deformation and feed rates $\dot{r}$ are depicted in Fig. 10. The MBN measurements confirm that the feed rate has no influence on the surface layer state, since the RMS value is also independent of the forming speed $\dot{r}$. For small radii up to 6 mm, the RMS value hardly changes. This can be caused by two different effects. On the one hand, the increasing degree of deformation increases the number of pinning sites in form of dislocations, which represent a barrier for domain wall movement and decrease the MBN activity (Fortuna et al., 2007). On the other hand, at low inner radii the existing collar height is not sufficient to cover the hole excitation coil and thus only a small volume is magnetized, which can also result in lower MBN signals. Despite the increasing dislocations density, decreasing the MBN signal, the RMS value shows a linear increase up to a radius of 9 mm. Due to a multidimensional stress state at the surface (see (Knoll et al., 2020)),it can be assumed that the present residual stresses have a negligible effect on the MBN compared to the microstructure, since the alignment of domain walls initiated by the

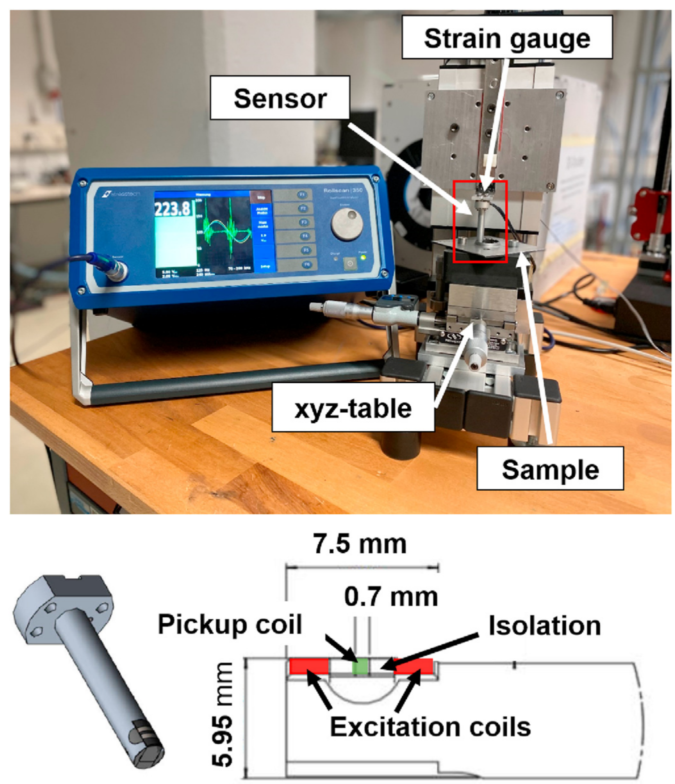

Fig. 9. Measurement setup for the punch-hole rolled samples (top) and a detailed view of the used Barkhausen-sensor geometry (bottom).

stress in a certain direction is compensated by the same effect in the other direction (Krause et al., 1999; Neslušan et al., 2018). Increasing RMS values at high plastification were also found in (Bayramoglu et al., 2010) and (Neslušan et al., 2018) where the influence of a HPT process and a severe shot peening on the MBN activity of steels was investigated and discussed. One factor, leading to higher RMS values, is the elongation of the grains inducing a reorientation of domain configuration and an increase of domain walls numbers.

As can be seen in Fig. 5c, the highly deformed banded grains are oriented in magnetization direction, and can therefore contribute to this effect. Furthermore a grain refinement, leading to smaller domain wall sizes and a higher amount of domain walls, increase the MBN activity as well. As deformation continues to increase, the Barkhausen activity

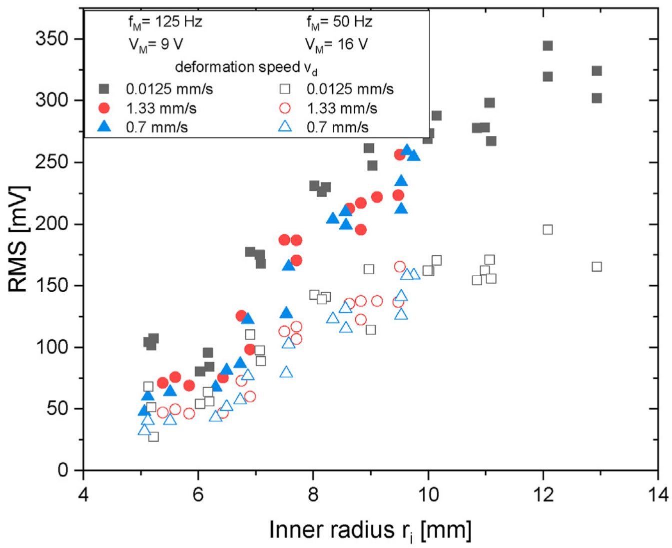

Fig. 10. Measured RMS value in dependence of the deformation speed v_d at different states of deformation and measuring parameters.

flattens, which correlates with occurring steady state in the hardness profile. This indicates, that the effect of grain refinement and elongation saturates and the effect of dislocations becomes more important again. The described effect can also be seen in Fig. 11, where the MBN envelope for different radii during a magnetization with the magnetization current I_M is shown. The increasing number of dislocation barriers s reflected by a shift of the peak position towards higher magnetization and also by a decrease of the FWHM. At higher degrees of deformation the envelopes resemble each other, indicating a uniformly deformed structure.

For the application of a MBN measuring system in a soft sensor concept, the integration into the process as well as the processing and analysis of the measured data plays a decisive role. A first approach for a workpiece model predicting the surface layer state based on MBN-measurements can be done by correlating the offline MBN data with the measured surface hardness. As can be seen in Fig. 12 on the left, the surface hardness shows a linear increase with higher RMS values. Thus the surface layer states represented in the hardness can be described by a linear measurement function. Since the MBN analysis is performed directly on the surface, an inline measurement during punch-hole-rolling can only be achieved if the sensor can be inserted into the tool. To clarify the question of whether the sensor must be in contact with the surface, as in the offline measurements, the influence of the sensor distance was investigated and the results are depicted in Fig. 12 (right). It is obvious that MBN activity drastically reduces by a non-contact measurement. Larger specimen diameters hereby cause a stronger decrease, since the smaller curvature has a stronger effect on the overall gap between sensor and surface. As a result, at a distance of 100 μm, the previously shown relationships between RMS value and radius (Fig. 10) no longer apply and the samples with the largest radius show the lowest RMS value. Thus, a contact must be ensured when integrating the sensor into the tool. The sensor integration into the tool with a simultaneous guarantee of a contact measurement could be achieved via a spring-mounted sensor unit that compensates for the process forces as well as surface fluctuations.

5. Conclusion and outlook

In this work, comprehensive process knowledge of punch-hole-rolling for the use in soft sensor models could be generated. Therein the correlations of the process parameters n and $\dot{r}$ with the process forces and the product geometry were presented. It was depicted that process forces increase with increasing feed rate $\dot{r}$, whereas the collar height shows a decreasing behavior. In contrast, the rotational speed n shows no significant influence on the process force or on the sample geometry. The induced surface layer state shows highly deformed UFG microstructure with an increase of hardness at about 80%. Hereby the variation of the process parameters did not affect the surface layer state at the same inner radii. Via offline MBN measurements it was possible to prove the suitability of a MBN sensor as a physical sensor in the soft sensor concept, predicting surface hardness as well as the induced grain size. In addition,

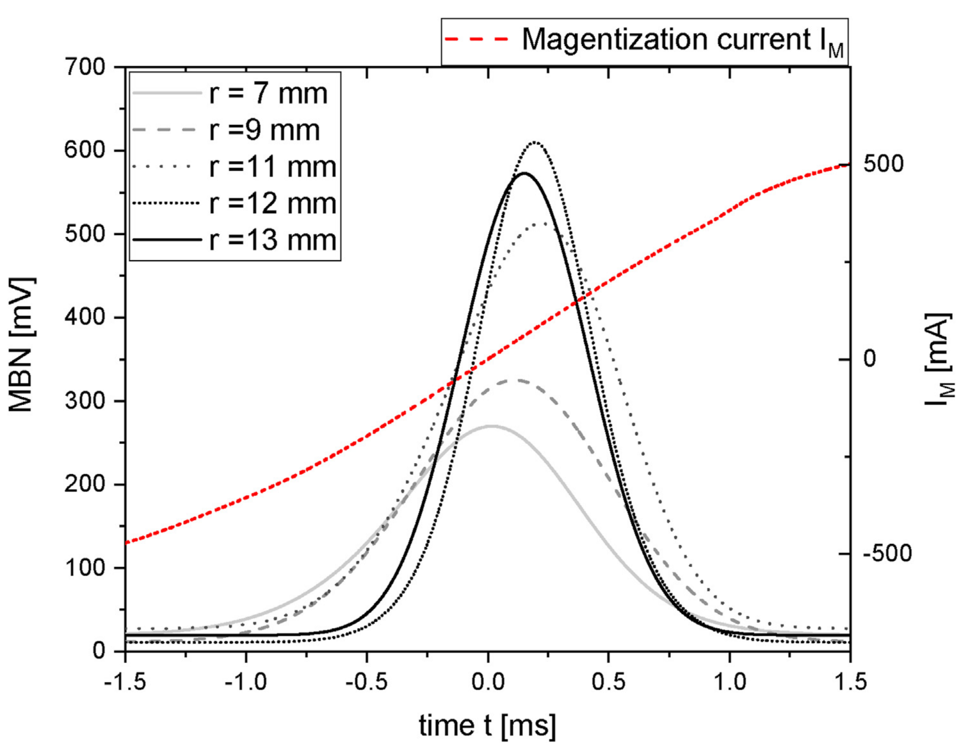

Fig. 11. Envelope of the MBN for different radii in dependence of the magnetization time with respect to the magnetization current I_M with 125 Hz.

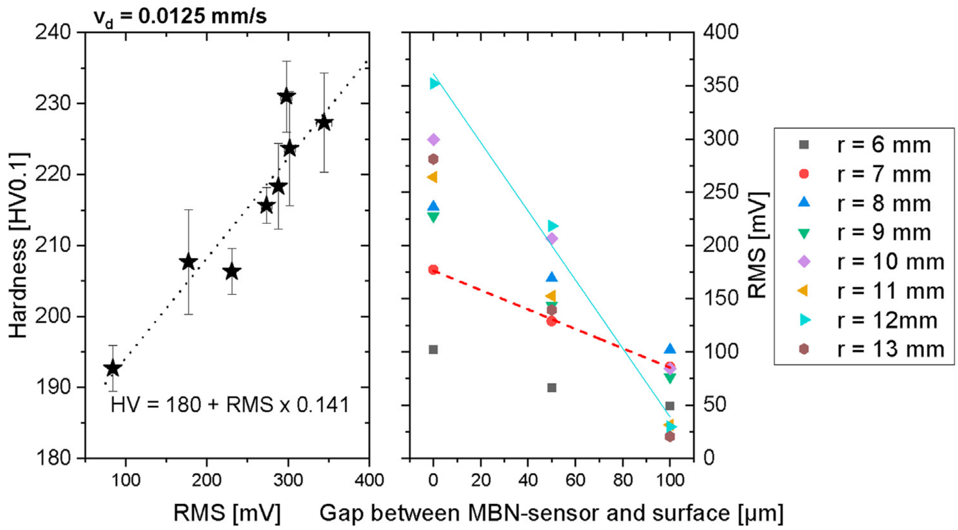

Fig. 12. Hardness 50 μm underneath the surface in dependence of the RMS value (left) and the influence of the distance between sensor and surface on the RMS value (right) measured at samples formed with a deformation speed $v_d = 0.0125 mms^{-1}$.

a first correlation between the MBN-signal and the surface could be established. Due to changing measurement conditions as a result of the increasing diameter, a measurement under contact is mandatory to make use of the derived relationships, challenging a sensor integration for an online application. Nevertheless the first steps in the design of a soft sensor for property controlled forming processes elaborate the most important aspects for the further development of this control technique. In particular, process parameters have to be further varied to exert more control over the surface layer state by controllable machine parameters.

Declaration of competing interest

The authors declare that they have no known competing financial interests or personal relationships that could have appeared to influence the work reported in this paper.

Acknowledgement

The authors would like to thank the German Research Foundation DFG for the support of the depicted research within the priority program 'SPP2183' through project no. 'GR 1818/721'. This work was partly carried out with the support of the Karlsruhe Nano Micro Facility (KNMF, www.knmf.kit.edu), a Helmholtz Research Infrastructure at Karlsruhe Institute of Technology (KIT, www.kit.edu).

References

Abu-Nabah, B.A., Yu, F., Hassan, W.T., Blodgett, M.P., Nagy, P.B., 2009. Eddy current residual stress profiling in surface-treated engine alloys. Nondestr. Test. Eval. 24 (1–2), 209–232.

Ahmad, I., Kano, M., Hasebe, S., Kitada, H., Murata, N., 2014a. Prediction of molten steel temperature in steel making process with uncertainty by integrating gray-box model and bootstrap filter. J. Chem. Eng. Jpn. 47 (11), 827–834.

Ahmad, I., Kano, M., Hasebe, S., Kitada, H., Murata, N., 2014b. Gray-box modeling for prediction and control of molten steel temperature in tundish. J. Process Contr. 24 (4), 375–382.

Ahmad, I., Ayub, A., Kano, M., Cheema, I.I., 2020. Gray-box soft sensors in process industry: current practice, and future prospects in era of big data. Processes 8 (2), 243.

Allwood, J., Duncan, S., Cao, J., Groche, P., Hirt, G., Kinsey, B., Kuboki, T., Liewald, M., Sterzing, A., Tekkaya, A., 2016. Closed-loop control of product properties in metal forming. CIRP Annals 65 (2), 573–596.

Baak, N., Nickel, J., Biermann, D., Walther, F., 2019. Barkhausen noise-based fatigue life prediction of deep drilled aisi 4140. Procedia Struct. Integr. 18, 274–279.

Bayramoglu, S., Gür, C.H., Alexandrov, I.V., Abramova, M.M., 2010. Characterization of ultra-fine grained steel samples produced by high pressure torsion via magnetic barkhausen noise analysis. Mater. Sci. Eng., A 527 (4–5), 927–933.

Boller, C., Altpeter, I., Dobmann, G., Rabung, M., Schreiber, J., Szielasko, K., Tschuncky, R., 2011. Electromagnetism as a means for understanding materials mechanics phenomena in magnetic materials. Mater. Werkst. 42 (4), 269–278.

Böttger, David, Stampfer, Benedict, Gauder, Daniel, Benjamin, Straß, Häfner, Benjamin, Lanza, Gisela, Schulze, Volker, Wolter, Bernd, 2020. Concept for soft sensor structure for turning processes of aisi4140: dfg priority program 2086, project: in-process soft sensor for surface-conditioning during longitudinal turning of aisi4140. In: Technisches Messen, –1 ahead-of-print.

Fortuna, L., Graziani, S., Rizzo, A., Xibilia, M.G., 2007. Soft sensors for monitoring and control of industrial processes. In: Advances in Industrial Control. London and Berlin and Heidelberg: Springer.

García-Martín, J., Gómez-Gil, J., Vázquez-Sánchez, E., 2011. Non-destructive techniques based on eddy current testing. Sensors (Basel, Switzerland) 11 (3), 2525–2565.

Gatelier-Rothea, C., Chicois, J., Fougeres, R., Fleischmann, P., 1998. Characterization of pure iron and (130p.p.m.) carbon–iron binary alloy by barkhausen noise measurements: study of the influence of stress and microstructure. Acta Materialia 46 (14), 4873–4882.

Groche, P., Vucic, D., Jöckel, M., 2007. Basics of linear flow splitting. J. Mater. Process. Technol. 183 (2), 249–255.

Heingärtner, J., Hora, P., 2011. Application of the eddy-current method in industrial car body production. In: Zero Failure Production Methods: Proceedings, pp. 83–87. May 17th-18th, 2011.

Jedamski, R., Heinzel, J., Rößler, M., Epp, J., Eckebrecht, J., Gentzen, J., Putz, M., Karpuschewski, B., 2020. Potential of magnetic barkhausen noise analysis for in-process monitoring of surface layer properties of steel components in grinding. TM - Tech. Mess. 87, no. 12.

Kadlec, P., Gabrys, B., Strandt, S., 2009. Data-driven soft sensors in the process industry. Comput. Chem. Eng. 33 (4), 795–814.

Knoll, M., Mühl, F., Groche, P., Schulze, V., 2020. Simulative basic investigation for a new forming process punch-hole-rolling. Procedia Manufac. 50, 503–509.

Krause, T.W., Mandal, K., Atherton, D.L., 1999. Modeling of magnetic barkhausen noise in single and dual easy axis systems in steel. J. Magn. Magn Mater. 195 (1), 193–205.

Le Manh, T., Benitez, J.A.P., Hernandez, J.H.E., Hallen López, J.M. (Eds.), 2020. Barkhausen Noise for Non-destructive Testing and Materials Characterization in Low Carbon Steels. Woodhead Publishing Series in Electronic and Optical Materials. Woodhead Publishing, Oxford.

Meurer, M., Tekkaya, B., Augspurger, T., Pullen, T., Schraknepper, D., Bergs, T., Münstermann, S., 2020. Cutting force based surface integrity soft-sensor when hard machining aisi 4140. TM - Tech. Mess. 87 (11), 683–693.

Müller, C., Bohn, T., Bruder, E., Bruder, T., Landersheim, V., el Dsoki, C., Groche, P., Veleva, D., 2007. Severe plastic deformation by linear flow splitting. Mater. Werkst. 38 (10), 842–854.

Mulrennan, K., Donovan, J., Creedon, L., Rogers, I., Lyons, J.G., McAfee, M., 2018. A soft sensor for prediction of mechanical properties of extruded pla sheet using an instrumented slit die and machine learning algorithms. Polym. Test. 69, 462–469.

Neslušan, M., Trško, L., Minárik, P., Čapek, J., Bronček, J., Pastorek, F., Čížek, J., Moravec, J., 2018. Non-destructive evaluation of steel surfaces after severe plastic deformation via the barkhausen noise technique. Metals 8 (12), 1029.

Ranjan, R., Jiles, D.C., Buck, O., Thompson, R.B., 1987. Grain size measurement using magnetic and acoustic barkhausen noise. J. Appl. Phys. 61 (8), 3199–3201.

Sakamoto, H., Okada, M., Homma, M., 1987. Theoretical analysis of barkhausen noise in carbon steels. IEEE Trans. Magn. 23 (5), 2236–2238.

Schmoeckel, D., Hauk, S., 2000. Tooling and process control for splitting of disk blanks. J. Mater. Process. Technol. 98 (1), 65–69.

Schulze, V., Zanger, F., Stampfer, B., Seewig, J., Uebel, J., Zabel, A., Wolter, B., Böttger, D., 2020. Surface conditioning in machining processes. TM - Tech. Mess. 87 (11), 661–673.

Sohlberg, B., 2005. Hybrid grey box modelling of a pickling process. Contr. Eng. Pract. 13 (9), 1093–1102.

Stefanita, C.-G. (Ed.), 2008. From Bulk to Nano: the Many Sides of Magnetism. Springer Berlin Heidelberg, Berlin, Heidelberg.

Zergoug, M., Lebaili, S., Boudjellal, H., Benchaala, A., 2004. Relation between mechanical microhardness and impedance variations in eddy current testing. NDT E Int. 37 (1), 65–72.

Žerovnik, P., Grum, J., 2009. Determination of residual stresses from the barkhausen noise voltage signal. In: 10th International Conference Of the Slovenian Society For Non-destructive Testing, pp. 437–445.